Investigational New Drugs (2019) 37:1117–1126
https://doi.org/10.1007/s10637-019-00738-y

PRECLINICAL STUDIES

Delineation of proapoptotic signaling of anthracene-shelled M_2L_4 metallacapsules and their synergistic activity with curcumin in cisplatin-sensitive and resistant tumor cell lines

Rositsa Mihaylova[1] · Anife Ahmedova[2] · Denitsa Momekova[3] · Georgi Momekov[1] · Nikolay Danchev[1]

Received: 7 December 2018 / Accepted: 31 January 2019 / Published online: 8 February 2019

Summary
Since the introduction of cisplatin into clinical practice a few decades ago, the topic of metal-based drugs has expanded significantly. Recent examples emphasize on metallosupramolecules as an emerging class of compounds with diverse properties. They can trigger unique cellular events in malignant cells or serve as molecular hosts for various biologically active compounds, including anticancer agents. The anthracene-shelled M_2L_4 coordination nanocapsules under research have already proved very high anticancer potency with remarkable selectivity and lack of cross-resistance. In this study, we provide an oncopharmacological evaluation of the Pt(II)- and Pd(II)-clipped M_2L_4 nanocapsules; we report a thorough analysis of their synergistic effects in combined treatments with the pleiotropic anticancer agent curcumin. We examined changes in cellular expression of several apoptosis-related proteins in a panel of tumor cell lines with different chemosensitivity towards cisplatin, i.e. HT-29, HL-60 and its resistant strains HL-60/CDDP and HL-60/Dox, in order to assess the molecular mechanisms of their antitumor activity The results of the immunoassay concluded activation of the mitochondrial apoptotic pathway in all the screened tumor lines. A prevalent modulation of the extrinsic apoptotic signaling cascade was observed in the chemoresistant variants. Curcumin interactions of the tested compounds were estimated against the cisplatin-refractory cell line HT-29 via the Chou-Talalay method (CTM), whereby the palladium species yielded superior synergistic activity as compared to their platinum analogues.

Keywords Metallosupramolecules · Synergism · Curcumin · Cisplatin resistance · Collateral sensitivity · Apoptosis

Introduction

Antitumor activity and safety profile of platinum-based drugs have been well explored in numerous clinical and research studies. The prototype metallodrug cisplatin is a key component of various chemotherapy regimens for treatment of advanced solid tumors (e.g. testicular teratoma, ovarian carcinoma, bladder carcinoma, among others). However, it has been ascribed a set of major limitations in terms of intrinsic or acquired resistance and pronounced off-target toxicity [1]. Renal damage, ototoxicity and severe emetogenicity are prominent dose-limiting side effects of cisplatin-based chemotherapy that often contribute to treatment failure [2]. Moreover, resistance to platinating agents can arise at any step of their mechanistic pathway due to cellular adaptation to stressful stimuli [3]. Therefore, recent studies are suggesting a more detailed classification of resistance related response mechanisms in respect of their sequence of emergence. Reduced cellular uptake via the copper transporter CTR1, active xenobiotic efflux and increased drug inactivation by cellular detoxifying enzyme systems are exemplary mechanisms of *pre-target resistance*. Target modifications that hinder drug interactions with DNA are plausible mechanisms of the *on-target resistance*. Finally, a plethora of miscellaneous mechanisms that interfere with recruitment of DNA lesion

✉ Georgi Momekov
gmomekov@gmail.com

[1] Department of Pharmacology, Pharmacotherapy and Toxicology, Faculty of Pharmacy, Medical University of Sofia, 2 Dunav Street, 1000 Sofia, Bulgaria

[2] Laboratory of Biocoordination and Bioanalytical Chemistry, Faculty of Chemistry and Pharmacy, "St. Kliment Ohridski" Sofia University, 1, J. Bourchier Blvd., 1164 Sofia, Bulgaria

[3] Department of Pharmaceutical Technology and Biopharmaceutics, Faculty of Pharmacy, Medical University of Sofia, 2 Dunav Street, 1000 Sofia, Bulgaria

repair machinery and apoptosis signaling pathways are cited to govern the emergence of *post-target resistance* [3–5]. While all three kinds of resistance may develop in parallel, a primary determinant of the MDR-resistant phenotype of numerous tumor types is the reduced intracellular drug accumulation [6, 7]. Overexpression of specific membrane transporters of the ATP-binding cassette (ABC) superfamily renders tumor cells resistant to a broad spectrum of chemically unrelated drugs (anthracylclines, vinca-alkaloids, podophyllotoxin derivatives, taxols etc.). Among them, the multidrug transporter ((MDR1) or P-glycoprotein (P-gp) coded by the ABCB1 gene appears to have the broadest substrate specificity and the widest tissues and organs distribution [8, 9]. Abnormal expression of MDR1 by some malignancies, such as colorectal carcinoma, is associated with innate resistance to various chemotherapy regimens. However, it has not been reported to play a pivotal role in resistance to cisplatin [4, 9]. Adversely, the ATP-dependent glutathione S-conjugate carrier ABCC2 of the multidrug resistance-associated proteins, namely MRP2, along with the copper exporting ATPases ATP7A and ATP7B have well been characterized as major CDDP-depleting efflux systems [3, 10, 11]. Although many studies report poor substrate affinity of the MRP1 (ABCC1) efflux transporter towards cisplatin, overexpression of MRP1 has been associated with cisplatin resistance in some types of cervical cancer. It has been recognized as a hallmark mechanism of MDR in acute myeloid leukemia (AML) [12]. The cross-resistance between cisplatin and its second generation derivative carboplatin had been another clinical challenge in treating patients with colorectal or ovarian cancer [13]. Therefore, much of drug development is aimed at improving the unfavorable pharmacological profile of conventional metallodrug. Novel approaches to a targeted drug delivery and controlled-release systems [14, 15] are pursued. As an emerging field of biomedicine, nanotechnology has rapidly advanced in constructing nanoscale delivery platforms with tunable physical and pharmacological properties (e.g. liposomes, dendrimers, nanoshells, nanotubes, etc.) [16]. While such host units can serve as drug vehicles for various bioactive molecules, they also carry unique mechanistic properties that are not attributed to the cargo itself [17].

The metallosupramolecular structures provide an interesting set of characteristics that can be employed in both cancer treatment and delivery of anticancer agents or bioimaging probes [18–20]. We have recently reported the excellent anticancer profiles of the Pt(II)- and Pd(II)- linked coordination nanocapsules in terms of high cytotoxicity and selectivity to cancer cells [21]. Furthermore, detailed studies indicated that they possess intrinsic antineoplastic potential and inhibit tumor cell growth equally well in chemosensitive, and de novo and ab initio resistant malignant cell lines [22]. Based on their peculiar, cisplatin-dissimilar chemical structure, potent tumor inhibiting properties and ability to bypass cross-resistance to conventional platinating agents, the Pt(II) and Pd(II) bisanthracene nanocapsules should be considered a new class of antineoplastic metallodrugs. Detailed studies on the importance and relevance of the chemical stability and guest-encapsulation state on the intrinsic anticancer activity of the capsules has suggested glutathione-triggered disassembly as a feasible activation pathway [22]. Glutathione (GSH) is recognized as the biomolecule relevant to cancer evolution as well as to drug resistance. This is why the proposed activation pathway corroborates with the observed high selectivity of these novel metallosupramolecules and with their ability to overcome drug resistance. Inspired by these findings, we started the current study to further elucidate the mechanistic aspects of the metallosupramolecular nanocapsules $\mathbf{1}^{\mathbf{Pt}}$ and $\mathbf{1}^{\mathbf{Pd}}$ (Fig. 1) We also hoped to evaluate their synergistic effects, following co-administration with the phytochemical curcumin, endowed with pronounced pleiotropic antineoplastic activity.

An alternative strategy for circumventing drug resistance and ameliorating dose-limiting toxicities of the conventional anticancer drugs is the combination chemotherapy [23]. Indeed, concomitant treatment regimens deliver superior antitumor efficacy as compared to monotherapy due to the synergistic effects of anticancer drugs of distinct, yet complementary modes of action. However, a drug combination may also exhibit additive or antagonistic effects that can be difficult to define and quantify [24]. Ting-Chao Chou and Paul Talalay have developed an applicable methodology (CTM, Chou-Talalay method) that is now widely acknowledged as a milestone in studying drug interactions [25]. Based on the median-effect principle, the CTM is a combination of the mass-action law and four other fundamental equations in biochemistry and biophysics, i.e. the Michaelis-Menten, Hill, Henderson-Hasselbalch and Scatchard equations [24, 26]. A computer software (CompuSyn®) performs an automated analysis of actual and simulated dose-response data and generates a plot of combination index (CI) values against different fractions affected (Fa). The CI provides a quantitative determination of a synergistic (CI < 1), additive (CI = 1), and antagonistic (CI > 1) drug behavior in fixed- or varying-ratio combinations. Similarly,

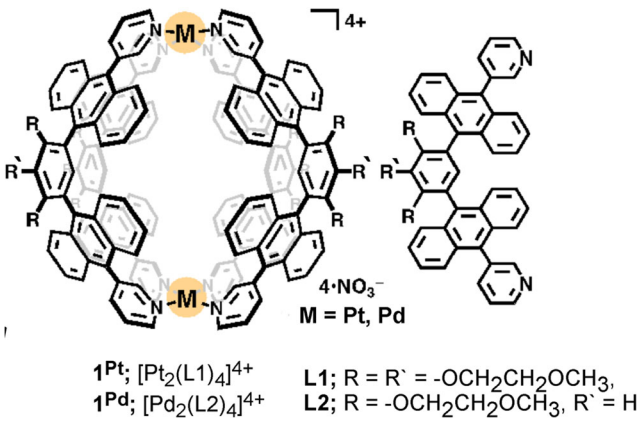

Fig. 1 Molecular structure of the Pt(II)- and Pd(II)- linked coordination nanocapsules $\mathbf{1}^{\mathbf{Pt}}$ and $\mathbf{1}^{\mathbf{Pd}}$, respectively

a DRI (dose reduction index)-Fa plot indicates the extent (folds) to which a single-drug dose may be reduced when used in a combination, without compromising the initial response it produced. Corresponding isobolograms are also constructed and can be used as an accessory tool in evaluating drug performance [24].

Materials and methods

Investigational compounds and instruments

Self-assembled isostructural Pt(II)- and Pd(II)-linked M_2L_4 coordination capsules, referred to as $\mathbf{1}^{\mathbf{Pt}}$ and $\mathbf{1}^{\mathbf{Pd}}$ in this text, were synthesized following previously reported procedures [27, 28]. Curcumin was obtained from Sigma-Aldrich Chemie GmbH, Germany (cat. No. C1386).

A multimode microplate reader Beckman Coulter DTX-880 was used to determine the MTT-formazan absorption at 580 nm. A Varian Cary Eclipse fluorimeter was used to measure the fluorescence spectra of supernatant of cancer cells treated with the capsules.

Cell lines and culture conditions

In vitro cytotoxicity was assessed in a panel of tumor cell lines of different chemosensitivity towards the prototype drug CDDP: cisplatin-refractory colorectal adenocarcinoma cells (HT-29); chemosensitive AML cell line (HL-60) and its correspondent cisplatin-resistant (HL-60/CDDP) and multidrug-resistant (HL-60/Dox) strains. The HL-60/CDDP subline was developed at the Laboratory of Experimental Chemotherapy (Faculty of Pharmacy, MU-Sofia). Selection has been carried out by prolonged serial exposures of the maternal cell line HL-60 to gradually increasing concentrations of CDDP. The established cisplatin-resistant phenotype has been sustained through cell cultivation in a growth medium containing 25 μM cisplatin. Resistant cells were incubated in a platinum-free environment at least five days prior to the experiment to avoid possible synergistic interactions with the compounds being screened for cytotoxicity. The multidrug-resistant derivative line HL-60/Dox was obtained from the German Cancer Research Center (DKFZ) in Heidelberg, Germany. The MDR-phenotype had been induced as specified above and has been sustained through cell cultivation in a growth medium containing 0.2 μM doxorubicin. Similarly, growth medium was to be cleared of the cytostatic drug not less than five days prior to the experiment. All other cell lines were purchased from the German Collection of Microorganisms and Cell Cultures (DSMZ GmbH, Braunschweig, Germany).

All cell cultures were cultivated in a growth medium RPMI 1640 supplemented with 10% fetal bovine serum (FBS), 5% L-glutamine and incubated under standard conditions of 37 °C and 5% humidified CO_2 atmosphere.

MTT dye reduction assay

Anticancer activity of the investigational nanocapsules was determined using a standard MTT-based colorimetric assay for evaluating cell viability. In brief, exponential-phased cells were harvested and seeded (100 μl/well) in 96-well plates at the appropriate density, i.e. 3×10^5 for suspension cultures (HL-60 and its derivatives) and 1.5×10^5 for the adherent one (HT-29). Following a 24 h incubation, cells were treated with serial dilutions of the tested substances in the concentration range of 100.00–0.20 μM. Following exposure time of 72 h, filter sterilized MTT substrate solution (5 mg/ml in PBS) was added to each well of the culture plate. A further 1–4-h incubation allowed formation of purple insoluble precipitates of the formazan dye. The latter were dissolved in isopropyl alcohol solution containing 5% formic acid prior to absorbance measurement at 550 nm. Collected absorbance values were blanked against MTT-and isopropanol solution and normalized to the mean value of untreated control (100% cell viability).

Statistical methods

Semi-logarithmic "dose-response" curves were computed using nonlinear regression in GraphPad Prism® 6.0. The cytostatic activity of the studied compounds was rated according to the calculated IC_{50} values (half maximal inhibitory concentrations).

Western blotting

The molecular basis of the antitumor activity of $\mathbf{1}^{\mathbf{Pt}}$ and $\mathbf{1}^{\mathbf{Pd}}$ was assessed via a series of western immunoblotting experiments. Each of the latter abided the following concise protocol: cell cultures at logarithmic phase of growth were seeded in 6-well plates at density of 3×10^5 and 1.5×10^5 for the suspension and adherent cells, respectively. Following a 24 h incubation, cells were treated with equi-effective concentrations of the studied compounds (i.e. IC_{50} and half of IC_{50}). After incubation time of 48 h cells were washed twice with ice-cold PBS, centrifuged at 3000 rpm for 6 min and cell pellets were stored at T = −80 °C until further analysis. Preserved probes were resuspended in a suspension buffer (0.58 *w/v* % NaCl, 0.16 w/v % Tris HCL, 0.04 w/v % EDTA) and aliquot samples were collected for protein quantification by the standard Pierce Protein Assay (PPA). Whole cell lysates were prepared with cell lysis buffer composed of 12.5 *v*/v % 1 M Tris HCL with pH = 6.8, 50 v/v % SDS (10% solution) and 25 v/v % Glycerol. During cell lysis samples were kept on ice in the presence of protease inhibitor (Complete Protease Inhibitor Cocktail Tablets, Roche®) to prevent proteins from degradation. Cell lysates were boiled at 100 °C for 5 min and subjected to SDS-PAGE electrophoresis. Seperated proteins were transfered onto a PVDF (polyvinylidene difluoride) membrane (transfer buffer composed of 0.3 *w/v* % Tris base, 1.4 w/v % Glycine, 0.1 w/v % SDS, 10 *v*/v % Methanol). Membranes

were blocked with 5% non-fat dry milk in TBS and incubated overnight at 4 °C with appropriate dilutions of primary antibodies against the protein of interest. Following 5-fold rinsing with washing solution (10 *v*/v % TBS, 0.1 v/v % Tween 20) secondary antibodies were added for a further 45 min. Visualization was performed with Luminol reagent (Santa Cruz Biotechnology Inc., Santa Cruz, California) and chemiluminescent signals were captured with X-ray films and quantified by densitometry (Bio-Rad® image analysis software).

Chou-Talalay method

The establishment and quantitative evaluation of the synergistic activity between the metal complexes and curcumin was based on the Chou-Talalay method and its respective CompuSyn® software. The "dose-response" relationships were derived in advance via the standard MTT test, following 72 h exposure to fixed-ratio combinations of the nanocapsules and curcumin in appropriate concentration ranges. To avoid any direct interactions between the studied compounds, cell treatment with curcumin was performed 2 h prior to that of $\mathbf{1}^{\mathbf{Pt}}$ and $\mathbf{1}^{\mathbf{Pd}}$. The experiment was conducted by varying the exposure time, exposure levels and molar ratios of curcumin and the nanocapsules with regard to the cytotoxic potential of the $\mathbf{1}^{\mathbf{Pt}}$ and $\mathbf{1}^{\mathbf{Pd}}$ analogues. Thereby, the fixed 1:10 (metal complex:curcumin) dose combination was selected as an optimal synergistic ratio for the platinum compound, whereas the 1:2 dose ratio was verified as the most effective protocol for the palladium derivatives. The nature of the drug interaction was determined based on the automatically calculated CI and DRI indices.

Results and discussions

Similarly to previously reported data, the MTT experiments showed far superior dose-dependent antineoplastic activity of $\mathbf{1}^{\mathbf{Pt}}$ and $\mathbf{1}^{\mathbf{Pd}}$ than the reference drug cisplatin in all tested cell lines. Calculated IC_{50} values vary within a narrow range of nano- and low micromolar concentrations (Table 1), as seen by the constructed "dose-response" curves in Fig. 2. However, $\mathbf{1}^{\mathbf{Pd}}$ inhibited cell growth markedly better in the suspension leukemic cell lines ($IC_{50,\ HL\text{-}60} = 1.6\ \mu M$, $IC_{50,\ HL\text{-}60/CDDP} = 0.7\ \mu M$, $IC_{50,\ HL\text{-}60/Dox} = 1.1\ \mu M$) as compared to the adherent malignant cells of epithelial origin HT-29 ($IC_{50,\ HT\text{-}29} = 3.5\ \mu M$). Conversely, the $\mathbf{1}^{\mathbf{Pt}}$ analogue demonstrated distinctly higher toxicity towards HT-29 ($IC_{50,\ HT\text{-}29} = 0.9\ \mu M$) than $\mathbf{1}^{\mathbf{Pd}}$. Although it is hard to draw such general conclusions regarding the chemosensitivity of the myeloid cell lines (closely comparable IC_{50} values), still one can imply that anticancer activity of the experimental capsules is slightly more pronounced in the cisplatin- and MDR-resistant variants. Indicating emergence of collateral sensitivity. We reason that such profound differences in tumor cell response to cisplatin and the novel metallosupramolecules may stem from mechanistic peculiarities of the latter linked to cell death induction or apoptosis evasion in malignant cells.

Table 1 In vitro cytotoxicity (mean IC_{50} values, [μM] ± SD) of $\mathbf{1}^{\mathbf{Pt}}$ and $\mathbf{1}^{\mathbf{Pd}}$ against HL-60, HL-60/CDDP, HL-60/Dox and HT-29 cells, compared with that of cisplatin

	Cisplatin	1^{Pt} *	1^{Pd}
HL-60	9.3 ± 3.7	5.0 ± 1.6	1.6 ± 0.3
HL-60/CDDP	13.2 ± 4.9	0.9 ± 0.4	0.7 ± 0.1
HL-60/Dox	32.9 ± 5.11	1.0 ± 0.2	1.1 ± 0.2
HT-29	36.6 ± 5.8	0.9 ± 0.1	3.5 ± 0.5

* Data from ref. 22

On one hand, the superior activity of the palladium counterparts in the chemoresistant HL-60/CDDP variant, and the thereof established collateral sensitivity phenomenon, could be ascribed to the biochemical properties of the metallacapsules, and on the other hand, on the molecular mechanisms underlying the resistance phenotype in these cells. In an earlier work we performed a thorough analysis of the biochemical features conditioning the resistance patterns in the established HL-60/CDDP sub-line [29]. Results of this survey concluded elevated glutathione levels, a ca. two fold increase in the activities of the GSH-associated antioxidant enzyme systems (glutathione-S-transferase, glutathione peroxidase, glutathione reductase) and an enhanced constitutive expression of the glutathione S-conjugate carrier MRP-1. In concert, the membrane transporter protein and its required co-substrate GSH mediate the unilateral efflux of GSH-adducts. The abundance of both detoxifying factors is associated with an extensive "pre-target" processing and depletion of the active platinum species. While this sum of adaptive cellular responses contributes to the observed decrease in susceptibility to classical platinum analogues, it is most probably accountable for the collateral sensitivity reported herein for the metal-coordinated capsules that are exemplary"rule-breakers". In a previous communication, we have shown that co-incubation of the platinum- and palladium-clipped nanocages with GSH leads to Pt-N bond cleavage and disassembly of the capsules, which are not capable of DNA-binding due to the lack of labile leaving groups [22]. However, both compounds greatly diverge in their rates of interaction with GSH – while the palladium capsule reacts immediately the platinum capsule is more inert and remains intact for more than 3 days. Thus, while serving as a molecular switch in resistance development, induction of GSH-related detoxifying pathways in HL-60/CDDP cells turned out to be a trigger factor in the "on-target" activation of the palladium species that showed strong growth inhibitory and apoptogenic effects in this cell line.

Identifying the capsules disassembly as the chemical process responsible for triggering their biological activity requires

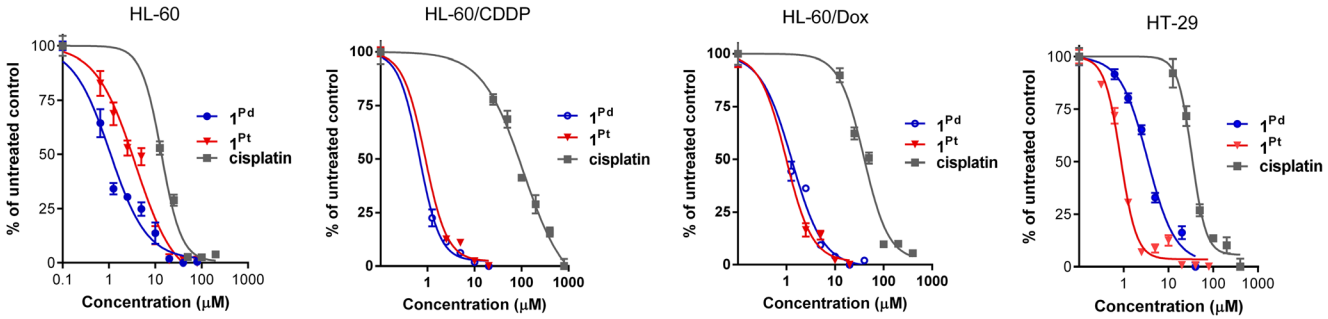

Fig. 2 "Dose-response" curves for HL-60, HL-60/CDDP, HL-60/Dox, HT-29 cell lines following 72 h exposure to $\mathbf{1}^{\mathbf{Pd}}$ (in blue) and $\mathbf{1}^{\mathbf{Pt}}$ (in red). Representative growth inhibition curves of cisplatin are shown in grey

closer study on this process, too. A very convenient and highly sensitive tool to assess the capsules stability is to monitor the fluorescence emitted by the free ligand **L**. The bisanthtracene ligands (**L1** and **L2**) show characteristic strong emission at ca. 440 nm, which is absent in the solutions of the capsules $\mathbf{1}^{\mathbf{Pt}}$ and $\mathbf{1}^{\mathbf{Pd}}$. These optical features have been used to monitor the stability of the capsules in complex media, such cellular milieu and presence of large biomolecules. Strong evidence for the high stability of the capsules in cellular milieu is demonstrated in Fig. 3 by the fluorescence spectra of supernatants of HL-60 cells treated with 10 μM solutions of the free ligand and the capsules $\mathbf{1}^{\mathbf{Pt}}$ and $\mathbf{1}^{\mathbf{Pd}}$ for 4 h. For this time period only negligible amount of the Pd(II) capsule decomposes and shows very weak fluorescence from the liberated ligand, whereas the Pt(II) capsule remains unchanged. The lack of fluorescence was also confirmed in our studies on the titration of buffer solutions of the capsules with salmon-sperm DNA solutions. Thereby, we confirm our previous observations that the main difference of the chemical reactivity of the Pt(II) and Pd(II) capsules is their reactivity rate with sulfur containing biomolecules, such as cysteine and glutathione, and is closely related to the known kinetic inertness of the Pt(II) pyridyl complexes in contrast to the more reactive Pd(II) ones.

In order to elucidate the mechanistic aspects underlying the tumor-inhibiting properties of the metal-coordinated nanocapsules we sought to determine their capacity to recruit specific signaling effects implicated in apoptotic cell death. To meet this objective, tumor cells were exposed to equi-effective concentrations of the tested compounds and thereafter the modulation of the target signaling cascades was established via Western-immunoblot. The specific molecular end-points were procaspase-8, procaspase-9, the pro-apoptotic factor bid of the bcl-2 family, and the xenobiotic transporter MRP1. The latter mediates the unilateral efflux of glutathione-conjugated xenobiotics from tumor cells, and has specifically been associated with MDR in HL-60/Dox.

As seen by the electrophoretic data presented in Fig. 4, the 24 h exposure of cells to $\mathbf{1}^{\mathbf{Pt}}$ and $\mathbf{1}^{\mathbf{Pd}}$ led to both agent- and cell

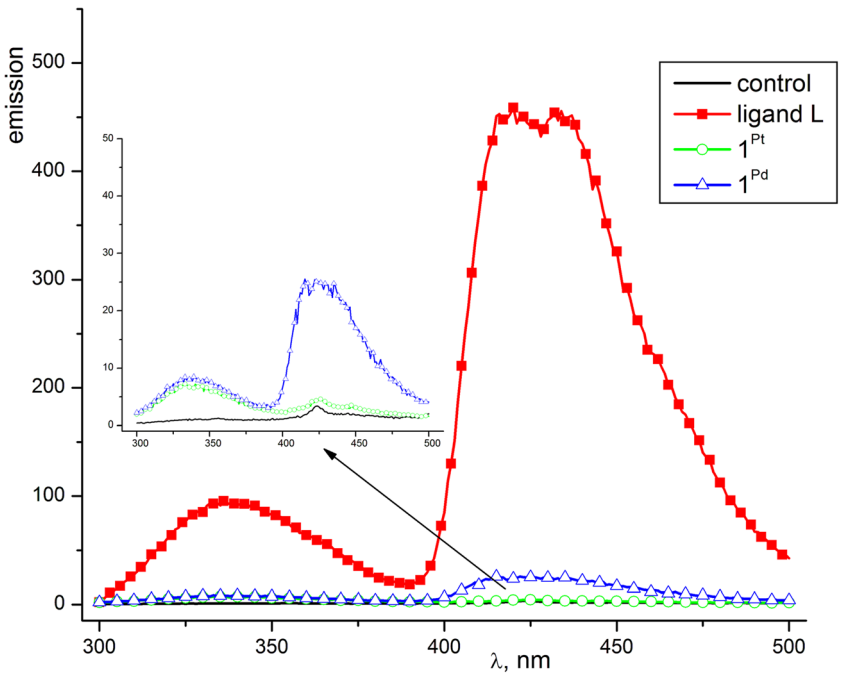

Fig. 3 Stability of the capsules $\mathbf{1}^{\mathbf{Pt}}$ and $\mathbf{1}^{\mathbf{Pd}}$ evidenced by the emission spectra of supernatants of HL-60 cells treated with 10 μM solutions of all compounds for 4 h (λ_{ex} = 260 nm). Ten-fold magnification is shown in the inset

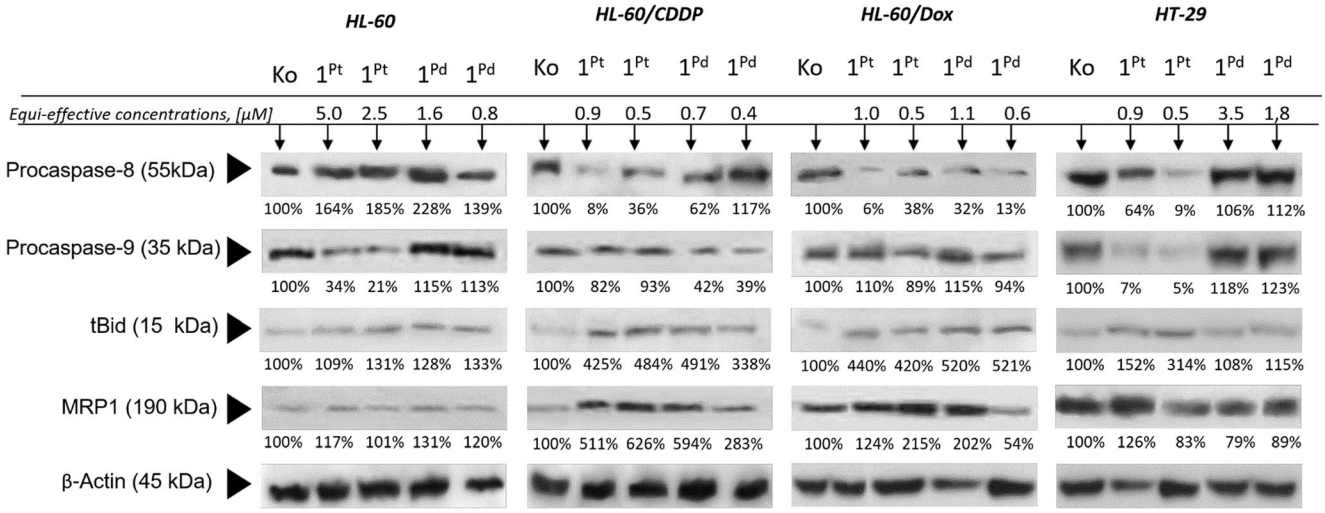

Fig. 4 Electrophoregram derived from the conducted Western blot experiments. Protein expression levels were measured by densitometric scanning of the band signals and normalized against β-actin. Treatment of HL-60, HL-60/CDDP, HL-60/Dox and HT-29 cells with equi-effective concentrations of $\mathbf{1}^{\mathbf{Pt}}$ and $\mathbf{1}^{\mathbf{Pd}}$ altered protein expression in a cell-line-, agent- and dose-specific manner and triggered alternative proapoptotic signaling pathways

line-specific patterns of activation of the intrinsic or extrinsic apoptotic pathways.

The induction of apoptosis by the platinum species in the chemosensitive cell line HL-60 proved to be mediated by the intrinsic pathway, as evidenced by the marked disappearance of the procaspase-9 band signal, indicative for its cleavage to the active protease form. In a dissimilar fashion, the palladium agent failed to induce activation of the intrinsic pathway in this cell line. Both novel compounds failed to recruit extrinsic apoptogenic signaling in HL-60, as attested by the lack of procaspase-8 cleavage.

In the cisplatin-resistant variant HL-60/CDDP the compounds triggered specific signaling events, whereby the platinum compound markedly activated caspase-8, whereas the palladium analogue cleaved the procaspase-8 only at the higher exposure level. It was found out that the platinum compound evoked less prominent activation of the intrinsic pathway in these cells. However, the palladium agent caused a significant disappearance of the procaspase-9 band in contrast to its lack of activity in the chemosensitive parent cell line.

In the multidrug-resistant tumor model HL-60/Dox both tested capsules caused significant activation of the extrinsic pathway with only marginal activation of the caspase-9-dependent mitochondrial apoptogenic cascade.

Juxtaposition of the electrophoretic signals in the HT-29 cancer cell line also demonstrates peculiar biological activities of the investigated agents. In this particular tumor model, the platinum analogue was a potent inducer of the extrinsic and intrinsic apoptotic pathways, whereas the palladium agent, albeit applied at equi-effective concentrations, failed to evoke cleavage of either procaspase zymogens.

Western blot readings for the pro-apoptotic factor bid of the bcl-2 family showed consistent findings in all the tested cell lines.

Table 2 CI and DRI indices calculated at actual experimental points

1^{Pt} + curcumin				1^{Pd} + curcumin			
Total dose	Fa	CI	DRI	Total Dose	Fa	CI	DRI
55.0	0.95	1.39740	0.84305	60.0	0.83	***0.59484***	***6.48271***
27.5	0.95	***0.69870***	***1.68610***	30.0	0.75	***0.45863***	***6.75411***
13.75	0.71	***0.91772***	***1.44155***	15.0	0.58	***0.47760***	***4.77987***
6.875	0.36	***0.95437***	***1.56655***	7.5	0.34	***0.66073***	***2.55275***
3.443	0.02	2.90620	0.79051	3.75	0.11	1.69264	0.75495

HT-29 cells were treated with 5-fold serial dilutions of $\mathbf{1}^{\mathbf{Pt}}$, $\mathbf{1}^{\mathbf{Pd}}$ and curcumin in the concentration range of 5–0.313 μM, 20–1.25 μM and 50–3.13 μM, correspondingly. Concomitant treatment with curcumin was performed in a fixed 1:10 and 1:2 (metal complex:curcumin) dose ratio within the indicated concentration ranges of $\mathbf{1}^{\mathbf{Pt}}$ and $\mathbf{1}^{\mathbf{Pd}}$, respectively. Thus, the total combination dose for the platinum species starts at 55.0 μM, and for the palladium analogue – at 60.0 μM. CI values <1 and DRI estimates >1 that are indicative of synergistic interactions are highlighted in bold italic

Table 3 CI and DRI estimates for data points of the simulated "dose-response" curve

A.	1^{Pt} + curcumin				B.		1^{Pd} + curcumin			
1^{Pt}	Curcumin	Total dose	CI	DRI	Fa	1^{Pd}	Curcumin	Total dose	CI	DRI
0.36652	3.72007	3.48292	1.71502	1.15757	**0.05**	0.30086	3.72007	1.53787	1.97943	0.58691
0.49968	6.30100	4.70688	1.53545	1.16775	**0.10**	0.81829	6.30100	2.71458	1.39301	0.90433
0.60537	8.73179	5.67164	1.44221	1.17409	**0.15**	1.52034	8.73179	3.85916	1.14076	1.18187
0.69945	11.1631	6.52642	1.37975	1.17889	**0.20**	2.42379	11.1631	5.02954	***0.99206***	1.44573
0.78809	13.6740	7.32875	1.33264	1.18287	**0.25**	3.56282	13.6740	6.25953	***0.89081***	1.70755
0.87467	16.3256	8.10997	1.29452	1.18636	**0.30**	4.98819	16.3256	7.57780	***0.81583***	1.97479
0.96152	19.1770	8.89145	1.26217	1.18953	**0.35**	6.77149	19.1770	9.01427	***0.75711***	2.25359
1.05057	22.2943	9.69071	1.23372	1.19291	**0.40**	9.01335	22.2943	10.6040	***0.70925***	2.55000
1.14371	25.7584	10.5245	1.20800	1.19538	**0.45**	11.8572	25.7584	12.3910	***0.66904***	2.87077
1.24297	29.6744	11.4111	1.18418	1.19819	***0.50***	15.5125	29.6744	14.4338	***0.63443***	3.22419
1.35085	34.1856	12.3723	1.16165	1.20101	**0.55**	20.2945	34.1856	16.8134	***0.60404***	3.62112
1.47060	39.4974	13.4369	1.13991	1.20390	**0.60**	26.6978	39.4974	19.6469	***0.57692***	4.07664
1.60681	45.9180	14.6447	1.11850	1.20691	**0.65**	35.5367	45.9180	23.1117	***0.55234***	4.61282
1.76636	53.9379	16.0559	1.09696	1.21014	**0.70**	48.2412	53.9379	27.4928	***0.52977***	5.26406
1.96041	64.3973	17.7674	1.07474	1.21371	**0.75**	67.5411	64.3973	33.2829	***0.50882***	6.08792
2.20885	78.8823	19.9517	1.05108	1.21781	**0.80**	99.2811	78.8823	41.4222	***0.48915***	7.19042
2.55214	100.846	22.9586	1.02477	1.22279	**0.85**	158.278	100.846	53.9845	***0.47057***	8.79576
3.09196	139.751	27.6644	***0.99334***	1.22943	**0.90**	294.073	139.751	76.7468	***0.45311***	11.4952
4.21526	236.708	37.3862	***0.94988***	1.24024	**0.95**	799.817	236.708	135.470	***0.43800***	17.7121

CI values <1 and DRI estimates >1 that indicate synergistic cytotoxic activity are highlighted in bold italic

Tumor cell exposure to $\mathbf{1^{Pt}}$ and $\mathbf{1^{Pd}}$ was invariably associated with cleavage of full-length bid to the active truncated form, namely tbid. It was notably more pronounced in the chemoresistant HL-60/CDDP and HL-60/Dox strains, as compared to their chemosensitive parent cell line HL-60. These findings well corroborate to the aforementioned superior procaspase-8 cleavage in the resistant models, as bid is well characterized as a downstream adapter molecule in the extrinsic apoptotic pathway recruited and activated by the very caspase-8.

There were some interesting findings regarding the expression of the xenobiotic efflux pump MRP1. In both chemosenstive and resistant leukemic cell lines, the 24 exposure to $\mathbf{1^{Pt}}$ and $\mathbf{1^{Pd}}$ was associated with increased levels of the ABC transporter, with the only exception being the palladium agent at the lower concentration in HL-60/Dox. Such an induction of MRP is most likely an adaptive stress response, which, however, compromises neither the cytotoxicity nor the apoptogenic properties of the novel compounds. Thereby, due to structural and mechanistic peculiarities of the $\mathbf{1^{Pt}}$ and $\mathbf{1^{Pd}}$ species, overexpression of the xenobiotic efflux pump in HL-60 cells does not seem to be relevant to their cytostatic properties. On the other hand, in the colorectal carcinoma cells HT-29 the palladium agent and the platinum analogue in the higher concentration caused a ca. 20% decrease in the expression level of the transporter molecule that may partly be accountable for the enhanced tumor responsiveness to the novel compounds.

Experimental data of the combination study were processed by means of computerized analysis based on the CTM and results of the generated report are summarized in the following tables.

As seen by the presented data, CI and DRI indices were generated not only for the actual viability data points (Tables 1 and 2), but also for each dataset of the simulated dose-response curve (Table 3) and the equi-effective concentrations IC_{50}, IC_{75}, IC_{90}, IC_{95} (Table 4).

According to the reported data in Table 3, the combination study for the platinum species established weak synergistic effects (CI < 1) with curcumin at only two of the computed "dose-response" datasets. They seem to correspond to the equivalent effective concentrations of IC_{90} and IC_{95},

Table 4 CI values at the equi-effective concentrations for both drug combinations

	ED_{50}	ED_{75}	ED_{90}	ED_{95}
CI (1^{Pt} + curcumin)	1.18418	1.07474	0.9933	0.94988
CI (1^{Pd} + curcumin)	0.63443	0.50882	0.45311	0.43800

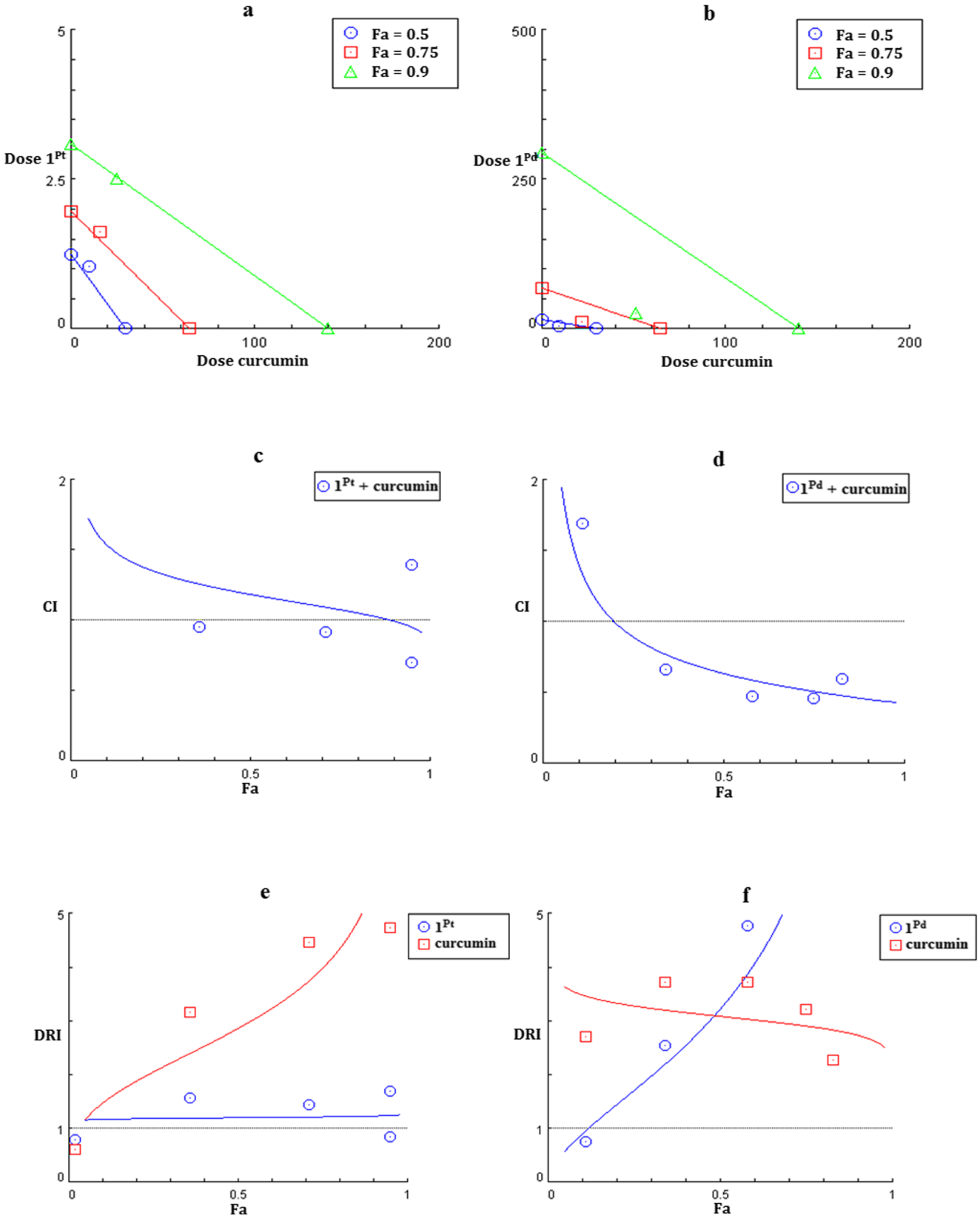

Fig. 5 Graphic representation of the combination study-derived end-points, namely: isobolograms (**a**, **b**), combination indices (**c**, **d**) and dose reduction indices (**e**, **f**) as a function of cell growth inhibition (see text for further details)

respectively (Table 4). However, a more pronounced synergistic trend was observed near the actual experimental points, whereat three out of the five estimated CI indices had a negative value (Table 2, Fig. 5c). The strongest synergistic effect (CI = 0.69870) exhibited the fixed-dose combination of 2.5 μM $\mathbf{1}^{\mathbf{Pt}}$: 25 μM curcumin that produced a total inhibitory effect of 95% (Table 2, Fa = 0.95), whereby the cited single drug concentrations lie near the IC_{50} values of both test compounds (Table 3, Fa = 0.5*)*. As shown in the isobologram of Fig. 5a, the pharmacodynamic interaction of $\mathbf{1}^{\mathbf{Pt}}$ with curcumin had an antagonistic effect at Fa = 0.5 (in blue), an additive one at Fa = 0.75 (in red) and yielded synergism at Fa = 0.9 (in green). The DRI calculations at the original experimental points (Table 2) well corroborate to these CI findings, with the second dataset having the highest DRI of approx. 1.7. Nonetheless, the DRI indices generated for the interpolated data points range near 1 and do not exceed 1.3 (Fig. 5e).

The overall evaluation of the drug interaction between the palladium nanocapsules and curcumin showed a greater consistency in synergistic behavior. Favorable CI values were estimated for most of the computed data points, whereby synergism is strongest immediately beyond the point of Fa = 0.50 (Table 3). Moreover, four out of the five experimental points for the palladium species yielded negative CI values with the lowest one corresponding to the drug ratio of 10 μM $\mathbf{1}^{\mathbf{Pd}}$: 20 μM curcumin at the Fa value of 0.75 (Table 2, Fig. 5d). These findings are partly in line with the synergy profile of the platinum analogue which too pointed out the second experimental data set as most effective. As indicated by the CI values in Table 4 and the isobologram in Fig. 5b, synergistic interaction between $\mathbf{1}^{\mathbf{Pd}}$ and curcumin occurs at all four equi-effective concentrations (IC_{50}, IC_{75}, IC_{90}, IC_{95}). Finally, the DRI indices for the palladium complex in the tested combination are well above 1 (Table 3), and thus assert a nearly 7-fold reduction of the initial single drug dose that practically remains equi-effective (Fig. 5f).

The fact that the synergistic combination with the palladium species delivered greater antitumor activity than their platinum counterparts deserves a special mention, since the HT-29 cells were far more susceptible to monotreatment with the platinum compound (Table 1). However, anticancer properties of curcumin against the colorectal carcinoma cell line are well documented, and its selective chemosensitization of HT-29 cells towards the $\mathbf{1}^{\mathbf{Pd}}$ derivatives may necessitate further mechanistic elucidation.

Conclusions

In continuation of our preceding studies on the bioinorganic chemistry and pharmacological properties of novel Pt(II)- and Pd(II)-clipped nanocapsules we,on one hand, provide a thorough mechanistic characterization of the intimate cell signaling events underlying the antineoplastic activity of the metal-based anthracene moieties. On the other hand, we demonstrate their capacity to synergistically augment the cytotoxic effects of the plant compound curcumin. The tested end-points include some crucial apoptogenic biomarkers such as caspase-8, caspase-9, and *bid*, as well as the drug-resistance associated ABC-transporter MRP-1. The findings of this study shed some light on the ability of the novel nanocapsules to inhibit malignant cells and aided to explain the mechanistic basis of the encountered collateral sensitivity in tumor cell lines with an acquired resistance or constitutively low responsiveness to chemotherapy. The tested compounds were attested as potent inducers of apoptosis, triggered by recruitment of the intrinsic pathway in all cellular test systems and associated with specific activation of the extrinsic caspase-8-dependent signaling cascade in the resistant tumor cell lines. The drug interaction investigation showed that both agents synergistically increased the efficacy of curcumin in HT-29 colon cancer cells, whereby the palladium analog demonstrated superior activity in terms of the combination indices (CI) values. These findings give us reason to consider $\mathbf{1}^{\mathbf{Pt}}$ and $\mathbf{1}^{\mathbf{Pd}}$ as exemplar compounds of a novel class of cytotoxic agents with prominent efficacy in chemotherapy-resistant tumor models. Moreover, the coordination metal center proved to be of foremost significance to the biological activity of the, albeit, isostructural metal complexes, as is evident from the specific cellular events evoked by both species.

Acknowledgements Assoc. Prof. Michito Yoshizawa, Dr. Masahiro Yamashina, and Prof. Munetaka Akita from Chemical Resources Laboratory of Tokyo Institute of Technology, Japan, are gratefully acknowledged for providing the coordination capsules, studied herein, and for their collaborative work in the past years**.** The National Science Fund of Bulgaria is gratefully acknowledged for the financial support (DFNI-B02/24).

Funding The work was supported by the The National Science Fund of Bulgaria through Grant contract No. DFNI-B02/24.

Compliance with ethical standards

Conflict of interest Rositsa Mihaylova declares that she has no conflict of interest. Anife Ahmedova declares that she has no conflict of interest. Denitsa Momekova declares that she has no conflict of interest. Georgi Momekov declares that he has no conflict of interest. Nikolay Danchev declares that he has no conflict of interest.

Ethical approval This article does not contain any studies with human participants or animals performed by any of the authors.

Informed consent For this type of study, formal consent is not required.

References

1. Boulikas T, Vougiouka M (2003) Cisplatin and platinum drugs at the molecular level (review). Oncol Rep 10:1663–1682. https://doi.org/10.3892/or.10.6.1663
2. Momekov G, Bakalova A, Karaivanova M (2005) Novel approaches towards development of non-classical platinum-based antineoplastic agents: Design of Platinum Complexes Characterized by an alternative DNA-binding pattern and/or tumor-targeted cytotoxicity. Curr Med Chem 12(19):2177–2191. https://doi.org/10.2174/0929867054864877
3. Galluzzi L, Vitale I, Michels J, Brenner C, Szabadkai G, Harel-Bellan A, Castedo M, Kroemer G (2014) Systems biology of cisplatin resistance: past, present and future. Cell Death Dis 5:e1257. https://doi.org/10.1038/cddis.2013.428
4. Galluzzi L, Senovilla L, Vitale I, Michels J, Martins I, Kepp O, Castedo M, Kroemer G (2012) Molecular mechanisms of cisplatin resistance. Oncogene 31(15):1869–1883. https://doi.org/10.1038/onc.2011.384
5. Shen DW, Pouliot LM, Hall MD, Gottesman MM (2012) Cisplatin resistance: a cellular self-defense mechanism resulting from multiple epigenetic and genetic changes. Pharmacol Rev 64(3):706–721. https://doi.org/10.1124/pr.111.005637
6. Sharom FJ (2014) Complex interplay between the P-glycoprotein multidrug efflux pump and the membrane: its role in modulating protein function. Front Oncol 4:41. https://doi.org/10.3389/fonc.2014.00041
7. Patel NR, Pattni BS, Abouzeid AH, Torchilin VP (2013) Nanopreparations to overcome multidrug resistance in cancer. Adv Drug Deliv Rev 65(13–14):1748–1762. https://doi.org/10.1016/j.addr.2013.08.004
8. Zinzi L, Capparelli E, Cantore M, Contino M, Leopoldo M, Colabufo NA (2014) Small and innovative molecules as new strategy to revert MDR. Front Oncol 4:2. https://doi.org/10.3389/fonc.2014.00002
9. Wu C-P, Hsieh C-H, Wu Y-S (2011) The emergence of drug transporter-mediated multidrug resistance to Cancer chemotherapy. Mol Pharm 8(6):1996–2011. https://doi.org/10.1021/mp200261n
10. Yamasaki M, Makino T, Masuzawa T, Kurokawa Y, Miyata H, Takiguchi S, Nakajima K, Fujiwara Y, Matsuura N, Mori M, Doki Y (2011) Role of multidrug resistance protein 2 (MRP2) in chemoresistance and clinical outcome in oesophageal squamous cell carcinoma. Br J Cancer 104(4):707–713. https://doi.org/10.1038/sj.bjc.6606071
11. Kilari D, Guancial E, Kim ES (2016) Role of copper transporters in platinum resistance. World J Clin Oncol 7(1):106–113. https://doi.org/10.5306/wjco.v7.i1.106
12. Zhu H, Luo H, Zhang W, Shen Z, Hu X, Zhu X (2016) Molecular mechanisms of cisplatin resistance in cervical cancer. Drug Des Devel Ther 10:1885–1895. https://doi.org/10.2147/DDDT.S106412
13. Matsuo K, Lin YG, Roman LD, Sood AK (2010) Overcoming platinum resistance in ovarian carcinoma. Expert Opin Investig Drugs 19(11):1339–1354. https://doi.org/10.1517/13543784.2010.515585
14. Wang X, Guo Z (2013) Targeting and delivery of platinum-based anticancer drugs. Chem Soc Rev 42(1):202–224. https://doi.org/10.1039/c2cs35259a
15. Zhou H, Wang G, Lu Y, Pan Z (2016) Bio-inspired cisplatin nanocarriers for osteosarcoma treatment. Biomater Sci 4(8):1212–1218. https://doi.org/10.1039/C6BM00331A
16. Piktel E, Niemirowicz K, Watek M, Wollny T, Deptula P, Bucki R (2016) Recent insights in nanotechnology-based drugs and formulations designed for effective anti-cancer therapy. J Nanobiotechnology 14(1):39. https://doi.org/10.1186/s12951-016-0193-x
17. Markman JL, Rekechenetskiy A, Holler E, Ljubimova JY (2013) Nanomedicine therapeutic approaches to overcome cancer drug resistance. Adv Drug Deliv Rev 65(13–14):1866–1879. https://doi.org/10.1016/j.addr.2013.09.019
18. Lewis JEM, Gavey EL, Cameron SA, Crowley JD (2012) Stimuli-responsive Pd_2L_4 metallosupramolecular cages: towards targeted cisplatin drug delivery. Chem Sci 3(3):778–784. https://doi.org/10.1039/c2sc00899h
19. Schmidt A, Hollering M, Drees M, Casini A, Kühn FE (2016) Supramolecular: Exo -functionalized palladium cages: fluorescent properties and biological activity. Dalton Trans 45(20):8556–8565. https://doi.org/10.1039/c6dt00654j
20. Therrien B (2012) Drug delivery by water-soluble organometallic cages. Top Curr Chem 319:35–55. https://doi.org/10.1007/128_2011_272
21. Ahmedova A, Momekova D, Yamashina M, Shestakova P, Momekov G, Akita M, Yoshizawa M (2016) Anticancer potencies of PtII-and PdII-linked M2L4 coordination capsules with improved selectivity. Chem Asian J 11(4):474–477
22. Ahmedova A, Mihaylova R, Momekova D, Shestakova P, Stoykova S, Zaharieva J, Yamashina M, Momekov G, Akita M, Yoshizawa M (2016) M_2L_4 coordination capsules with tunable anticancer activity upon guest encapsulation. Dalton Trans 45(33):13214–13221. https://doi.org/10.1039/C6DT01801G
23. Pinto AC, Moreira JN, Simões S (2011) Combination chemotherapy in Cancer: principles, evaluation and drug delivery strategies. Current Cancer treatment – novel beyond conventional approaches. InTech, Available from: http://www.intechopen.com/books/current-cancer-treatment-novel-beyond-conventional-approaches/combination-chemotherapy-in-cancer-principles-evaluation-and-drug-delivery-strategie. Accessed August 2018
24. Chou TC (2006) Theoretical basis, experimental design, and computerized simulation of synergism and antagonism in drug combination studies. Pharmacol Rev 58(3):621–681. https://doi.org/10.1124/pr.58.3.10
25. Chou TC, Talalay P (1984) Quantitative analysis of dose-effect relationships: the combined effects of multiple drugs or enzyme inhibitors. Adv Enzym Regul 22:27–55
26. Chou TC (2010) Drug combination studies and their synergy quantification using the Chou-Talalay method. Cancer Res 70(2):440–446. https://doi.org/10.1158/0008-5472.CAN-09-1947
27. Kishi N, Li Z, Yoza K, Akita M, Yoshizawa M (2011) An M_2L_4 molecular capsule with an anthracene Shell: encapsulation of large guests up to 1 nm. J Am Chem Soc 133(30):11438–11441. https://doi.org/10.1021/ja2037029
28. Yamashina M, Sei Y, Akita M, Yoshizawa M (2014) Safe storage of radical initiators within a polyaromatic nanocapsule. Nat Commun 5:4662. https://doi.org/10.1038/ncomms5662.
29. Zhelezova I, Momekov G, Konstantinov S In vitro models of drug resistance in AML cell lines. In: Pajeva I, Argirova R, Bacvarov K, Boteva D, Burneva N (eds) Bulgarian-German scientific cooperation: past, present and future., Sofia, November 26–28, 2015. Humboldt Union in Bulgaria, pp 166–171